Anti-Inflammatory Effect of Dexamethasone Controlled Released From Anterior Suprachoroidal Polyurethane Implants on Endotoxin-Induced Uveitis in Rats

Juliana Barbosa Saliba,[1–4] Lorena Vieira,[1–4] Gabriella Maria Fernandes-Cunha,[1–4] Gisele Rodrigues Da Silva,[5] Sílvia Ligório Fialho,[6] Armando Silva-Cunha,[1] Elodie Bousquet,[2–4] Marie-Christine Naud,[2–4] Eliane Ayres,[7] Rodrigo Lambert Oréfice,[8] Meriem Tekaya,[9] Laura Kowalczuk,[9] Min Zhao,[2–4] and Francine Behar-Cohen[2–4,9]

[1]Faculty of Pharmacy, Federal University of Minas Gerais, Belo Horizonte, Minas Gerais, Brazil
[2]Inserm UMR_S 1138, Team 17: From Physiopathology of Retinal Diseases to Clinical Advances, Centre de Recherche des Cordeliers, Paris, France
[3]Sorbonne Universities, University of Pierre et Marie Curie, Centre de Recherche des Cordeliers, Paris, France
[4]Paris Descartes University, Sorbonne Paris Cité, Centre de Recherche des Cordeliers, Paris, France
[5]School of Pharmacy, Federal University of São João Del Rei, Divinópolis, Minas Gerais, Brazil
[6]Pharmaceutical and Biotechnological Development, Ezequiel Dias Foundation, Belo Horizonte, Minas Gerais, Brazil
[7]State University of Minas Gerais, Belo Horizonte, Minas Gerais, Brazil
[8]Department of Metallurgical and Materials Engineering, Federal University of Minas Gerais, Belo Horizonte, Minas Gerais, Brazil
[9]Department of Ophthalmology of University of Lausanne, Jules-Gonin Ophthalmic Hospital, CHUV, Lausanne, Switzerland

Correspondence: Min Zhao, INSERM UMR_S 1138, Team 17, Centre de Recherche des Cordeliers, 15 rue de l'Ecole de Médecine, 75006, Paris, France;
min.zhao@inserm.fr.

MZ and FB-C are joint senior authors.

Submitted: September 5, 2015
Accepted: February 27, 2016

Citation: Barbosa Saliba J, Vieira L, Fernandes-Cunha GM, et al. Anti-inflammatory effect of dexamethasone controlled released from anterior suprachoroidal polyurethane implants on endotoxin-induced uveitis in rats. *Invest Ophthalmol Vis Sci*. 2016;57:1671–1679. DOI:10.1167/iovs.15-18127

Purpose. Targeted drug delivery to the ocular tissues remains a challenge. Biodegradable intraocular implants allow prolonged controlled release of drugs directly into the eye. In this study, we evaluated an anterior suprachoroidal polyurethane implant containing dexamethasone polyurethane dispersions (DX-PUD) as a drug delivery system in the rat model of endotoxin-induced uveitis (EIU).

Methods. In vitro drug release was studied using PUD implants containing 8%, 20%, and 30% (wt/wt) DX. Cytotoxicity of the degradation products of DX-PUD was assessed on human ARPE-19 cells using 3-(4,5-dimethylthiazolyl-2)-2,5-diphenyltetrazolium bromide (MTT) test. Short-term ocular biocompatibility of suprachoroidal DX-PUD implants was evaluated in normal rat eyes. Endotoxin-induced uveitis was then induced in rat eyes preimplanted with DX-PUD. Clinical examination was performed at 24 hours; eyes were used to assess inflammatory cell infiltration and macrophage/microglial activation. Cytokine and chemokine expression in the iris/ciliary body and in the retina was investigated using quantitative PCR. Feasibility of anterior suprachoroidal PUD implantation was also tested using postmortem human eyes.

Results. A burst release was followed by a sustained controlled release of DX from PUD implants. By-products of the DX-PUD were not toxic to human ARPE-19 cells or to rat ocular tissues. Dexamethasone-PUD implants prevented EIU in rat eyes, reducing inflammatory cell infiltration and inhibiting macrophage/microglial activation. Dexamethasone-PUD downregulated proinflammatory cytokines/chemokines (IL-1β, IL-6, cytokine-induced neutrophil chemoattractant [CINC]) and inducible nitric oxide synthase (iNOS) and upregulated IL-10 anti-inflammatory cytokine. Polyurethane dispersion was successfully implanted into postmortem human eyes.

Conclusions. Dexamethasone-PUD implanted in the anterior suprachoroidal space may be of interest in the treatment of intraocular inflammation.

Keywords: polyurethane, implant, suprachoroidal space, drug delivery, endotoxin-induced uveitis

The treatment of intraocular inflammation, such as anterior, intermediate, and/or posterior uveitis, requires therapeutic concentrations of drugs for a prolonged period. However, ocular static barriers (cornea, sclera, blood–aqueous and blood–retinal barriers) and ocular dynamic barriers (tear dilution, conjunctival and choroidal blood flow),[1] as well as efflux pumps, limit the drug access to ocular tissues.[2]

Recently, intraocular implants based on biodegradable and nonbiodegradable polymers incorporating drugs have been used to treat ocular diseases. The nonbiodegradable implantable devices containing ganciclovir or fluocinolone acetonide (Vitrasert and Retisert, respectively; Bausch & Lomb, Rochester, NY, USA) have been approved for the treatment of cytomegalovirus retinitis and chronic noninfectious posterior uveitis,

Investigative Ophthalmology & Visual Science

respectively. The biodegradable implants composed of poly(-lactic-co-glycolic acid) and dexamethasone (DX) (Ozurdex; Allergan, Irvine, CA, USA) have also been approved for the treatment of persistent macular edema following retinal vein occlusion, diabetic macular edema, and noninfectious posterior uveitis.[3–5] These implants release therapeutic concentrations of the drugs into the target site for a prolonged period, overcome the natural ocular barriers, and reduce systemic side effects, although glucocorticoid-incorporated delivery systems may cause cataract and intraocular pressure elevation.[6–8]

Developing minimally invasive and long-acting intraocular implants based on biodegradable polymers is the focus of research for the treatment of the vitreoretinal disorders.[9] Suprachoroidal space (SCS) provides a large potential anatomic space for drug delivery. Suprachoroidal injection has shown a significant improvement of drug transport only to adjacent tissues, the choroid and retina, in animal models when compared with intravitreal and subconjunctival administration.[10–12] Implants composed of biodegradable polyurethane were previously elaborated on, and we demonstrated their ocular biocompatibility, as they induce neither inflammatory responses in the eye nor alterations of the retinal architecture.[13] We previously showed that polyurethane implants releasing DX inhibited local inflammatory response and angiogenesis in a murine model for a prolonged period.[14]

In this study, we demonstrate the ocular biocompatibility of DX-loaded polyurethane implants and of their degradation products. These implants can be successfully inserted into the supraciliary space or into the SCS facing either the posterior or peripheral retina of rat eyes and human eyes. A polyurethane thin sheet containing DX implanted in the anterior SCS prevents ocular inflammation in rat endotoxin-induced uveitis, a model of acute anterior uveitis affecting also the posterior segment. Biocompatible and biodegradable polyurethane suprachoroidal implants could be used as targeted drug delivery systems for ocular diseases.

Methods

Preparation of Dexamethasone-Loaded Polyurethane Implants

Aqueous polyurethane dispersions (PUD) were prepared as previously described.[15] This chemical procedure was successful in producing polyurethane dispersions with solid content of approximately 20%. The composition of the PUD is shown in Table 1. Polymeric films were produced by casting the dispersions in a Teflon mold and allowing them to dry at room temperature for 1 week. Films were then placed in an oven at 60°C for 24 hours. Different amounts of DX (Sigma-Aldrich, Saint Quentin Fallavier, France) (6.0, 18.8, and 29 mg) were incorporated into the polymer by dispersing them in 2 mL PUD prior to casting the films to yield materials having 8%, 20%, or 30% (wt/wt) of the drug. The dried sheet-like films (Fig. 1A, approximately 0.2-mm thickness) were cut to obtain the DX-loaded polyurethane implants (DX-PUD sheets). Blank PUD implants were also prepared (PUD sheets).

In Vitro Release of DX From the PUD Sheets

Polyurethane dispersion sheets (Fig. 1A) loaded with different concentrations of DX (8%, 20%, or 30%, wt/wt) were placed in 24-well tissue culture plates (BD Falcon, Le Pont de Claix, France) containing 2.0 mL phosphate-buffered saline (PBS, pH 7.4) at 37°C ($n = 6$ for each sample). From day 1 to 7, the PBS was totally retrieved daily, then every week until day 42. At each time point, after PBS collection, the same volume of fresh PBS was added to the well. The amount of DX released from the PUD sheets was assayed by high-performance liquid chromatography and expressed as the cumulative percentage of DX leached in the PBS. The average of the obtained measurements was calculated and used to plot the release profile curve.

Table 1. Composition of the Aqueous Polyurethane Dispersion

Reagents	Concentration, % wt/wt
Isophorone diisocyanate (IPDI)	8.58
Polycaprolactone-diol1000 (PCL1000)	4.85
Polycaprolactone-diol2000 (PCL2000)	8.36
Polyethylene glycol (PEG1500)	0.73
2, 2-bis(hydroxymethyl) propionic acid (DMPA)	0.97
Triethylamine (TEA)	0.73
Water	74.70
Hydrazine (HZ)	1.08

Fourier Transform Infrared Spectroscopy Analysis of the Degraded PUD Sheets

Blank PUD sheets were placed in 24-well tissue culture plates containing 2.0 mL PBS at 37°C for 20 and 60 days ($n = 6$ for each time point). After these periods, degraded PUD sheets were collected, and the excess surface water was removed using filter paper. Then, PUD sheets were maintained in a desiccator at room temperature for 14 days for water evaporation. The samples were analyzed by Fourier transform infrared spectrophotometer (FTIR) (Perkin Elmer Spectrum 1000; Saint Paul, MN, USA) using the attenuated total reflectance (ATR) technique. Each spectrum was a result of 32 scans with a resolution of 4 cm^{-1}. The initial PUD sheets were also analyzed.

ARPE-19 Cell Culture

ARPE-19 cells were cultured in Dulbecco's modified Eagle's medium and Ham's F12 medium (DMEM/F12; Life Technologies, Saint-Aubin, France) containing 10% fetal bovine serum (FBS), and incubated in a humidified atmosphere of 5% CO_2 and 95% air at 37°C.

In Vitro Cytotoxicity of the Degradation Products of the DX-PUD Sheets

After sterilization with UV lights for 45 minutes each side, DX-PUD sheets (30% wt/wt, 30-mm^2 surface area) were incubated with 3 mL PBS at 37°C for 4 months. Phosphate-buffered saline containing the degradation products of DX-PUD was then collected. ARPE-19 cells were seeded at 4×10^5/well in 24-well tissue culture plates. Upon confluence, cells were treated with

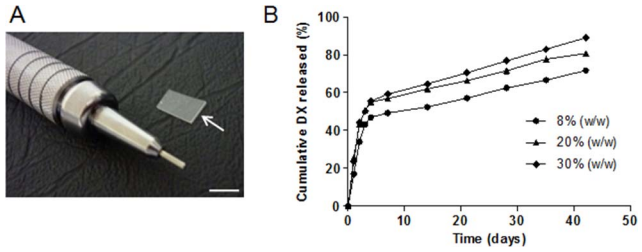

Figure 1. PUD implant sheet ([**A**], *arrow*) and in vitro release profiles of PUD containing 8%, 20%, or 30% (wt/wt) of the DX ($n = 6$ samples for each point [**B**]). The relative standard deviation of all data is lower than 7%. *Scale Bar*: 5 mm (**A**).

a mixture of fresh culture medium with PBS containing degradation products (10:1). Control cells were incubated with culture medium containing fresh PBS. After 1 and 4 days, cell viability was evaluated using 3-(4,5-dimethylthiazolyl-2)-2,5-diphenyltetrazolium bromide (MTT) assay (Sigma-Aldrich) according to manufacturer's instructions. Experiments were performed in quadruplicate. The result was expressed as a percentage relative to the control cells.

Animals

Female Lewis rats (6–8 weeks old; Janvier, Le Genest-Saint-Isle, France) were kept in pathogen-free conditions with food and water ad libitum and housed in a 12-hour light/12-hour dark cycle. All animal experiments were performed in accordance with the ARVO Statement for the Use of Animals in Ophthalmic and Vision Research and approved by the ethical committee of Paris Descartes University (ID Ce5/2012/122). Anesthesia was induced by intramuscular ketamine (50 mg/kg) and xylazine (3 mg/kg). Drops of 1% tetracaine were used for topical anesthesia.

Implantation of DX-PUD Sheets in the SCS of Rat Eyes and in the Supraciliary Space of Postmortem Human Eyes

Sterilized PUD sheets (containing 8%, 20%, or 30% DX) of 1 × 5 mm were cut under a surgical microscope. After anesthesia, the conjunctiva of the rat eye was opened in the superior temporal quadrant. For suprachoroidal implantation, a 2-mm full-thickness sclera incision was performed vertically and at 4 mm from the limbus. A tunnel 5 mm long was made between the sclera and the choroid and parallel to the limbus using a 25-gauge needle. A PUD sheet was then slid inside the SCS. No scleral or conjunctival suture was needed. Polyurethane dispersion sheets were also implanted in the anterior SCS at 1 mm from the limbus. Localization of the polymeric implant was further examined in vivo using spectral-domain optical coherence tomography (SD-OCT; Spectralis device; Heidelberg Engineering, Heidelberg, Germany) adapted for small animals.

We also implanted PUD sheets in the supraciliary space in two postmortem human eyes. The eyes were collected for research purposes at 13 hours post mortem in conformity with the Swiss Federal law on transplantation. All procedures conformed to the tenets of the Declaration of Helsinki for biomedical research involving human subjects. A full-thickness scleral incision was made at 4 mm from the limbus; PUD implants (2 mm × 2 cm) were then inserted gently into the supraciliary space.

Endotoxin-Induced Uveitis

Endotoxin-induced uveitis (EIU) is a well-characterized rat model for human acute uveitis.[16] To evaluate the effect of DX-PUD implants on EIU, the disease was induced 15 days after the implantation of the device by a single footpad injection of 100 μL sterile pyrogen-free saline containing 200 mg lipopolysaccharide (LPS) from *Salmonella typhimurium* (Sigma-Aldrich). The animals received also blank PUD implants. Subconjunctival injection of 20 μg DX[17] and intravitreal injection of 0.25 μg DX served as positive controls.

Clinical Examination

Twenty-four hours after LPS challenge, rat eyes were examined using slit-lamp. The intensity of inflammation was classified from grade 0 to grade 5 as previously described.[18] Scoring was performed by a masked investigator. Rats were then killed and eyes enucleated for histology, immunofluorescence, and real-time PCR analyses.

Histology

Rat eyes were fixed in 4% paraformaldehyde (PFA) and 0.5% glutaraldehyde for 2 hours, dehydrated in a graded alcohol series, and embedded in historesin (Leica, Heidelberg, Germany). Sections of 5 μm were obtained using a Leica Jung RM2055 microtome and stained with 1% toluidine blue. Polymorphonuclear (PMN) cells, identified by the shape of their nuclei, were quantified on histologic sections. The analysis was performed on seven rats (seven eyes) per experimental group with four different sections per eye at the optic nerve head level.

Human eyes were fixed in formalin for 1 day. The posterior segment of the eye was then removed. The remaining anterior segment was fixed in formalin for 2 more days, then dehydrated in alcohol and embedded in paraffin using a tissue processor (Citadel 2000, Shandon, Thermo Scientific, Reinach, Switzerland). Sections of 5 μm were stained with hematoxylin and eosin.

Immunofluorescence

Eyes were fixed in 4% PFA and incubated with a graded series of sucrose before being snap frozen in Tissue-Tek optimal cutting temperature (OCT) compound (Bayer Diagnostics, Puteaux, France). The following primary antibodies were used on cryosections: mouse anti-ED1 (1:50; AbDSerotec, Colmar, France), mouse anti-inducible nitric oxide synthase (iNOS, 1:75; Santa Cruz Biotechnology, Heidelberg, Germany), and rabbit anti-ionized calcium binding adaptor molecule-1 (anti-IBA-1, 1:400; Wako, Richmond, VA, USA). The secondary antibodies (Life Technologies) were Alexa Fluor 488–coupled goat anti-mouse IgG (1:200), Alexa Fluor 594–coupled goat anti-mouse IgG (1:200), and Alexa Fluor 488–coupled goat anti-rabbit IgG (1:200). Negative controls were performed by omission of primary antibody. ED1-positive macrophage infiltration in EIU rat eyes was quantified on cross sections at the optic nerve head level. Four eyes from four rats per group and four sections per eye were analyzed.

Reverse Transcription and Real-Time PCR

Total RNA was isolated from iris/ciliary body or from neuroretina using RNeasy plus Mini Kit (Qiagen, Courtaboeuf, France). First-strand cDNA was synthesized using random primers (Life Technologies). Transcription levels of tumor necrosis factor-α (TNF-α), interleukin 1β (IL-1β), interleukin 6 (IL-6), interleukin 10 (IL-10), cytokine-induced neutrophil chemoattractant (CINC), iNOS, and occludin (Table 2) were analyzed by real-time PCR performed in the 7500 Real-Time PCR System (Applied Biosystems, Foster City, CA, USA) with either Taqman or SYBR Green detection. The hypoxanthine phosphoribosyltransferase (HPRT) was used as internal control. Delta cycle threshold calculation was used for relative quantification of results.

Statistical Analysis

Data are expressed as the mean ± SE. Statistical analysis was performed using GraphPad Prism 5 (GraphPad Software, Inc., San Diego, CA, USA). Kruskal-Wallis test followed by Dunn's comparison was used. Values of $P < 0.05$ were considered significant.

Results

In Vitro Release of the DX From the PUD Sheets

Dexamethasone was released in vitro from PUD sheets containing different concentrations of the drug (8%, 20%, or 30%, wt/wt) during 42 days (Fig. 1B). The release profiles were

Table 2. Real-Time PCR Primers and Probes

Gene	Primer and TaqMan Probe Reference
HPRT1	Rn01527840_m1
TNF-α	Rn01525859-g1
IL-1β	Rn00676333_g1
IL-6	Rn01410330_m1
iNOS	Rn00561646-m1
	SYBR Green primer
HPRT1	
Sense	5′-GCGAAAGTGGAAAAGCCAAGT-3′
Antisense	5′-GCCACATCAACAGGACTCTTGTAG-3′
IL-10	
Sense	5′-CCTCTGGATACAGCTGCGAC-3′
Antisense	5′-GTAGATGCCGGGTGGTTCAA-3′
CINC	
Sense	5′-GGGTGTCCCCAAGTAATGGA-3′
Antisense	5′-CAGAAGCCAGCGTTCACCA-3′

similar for all DX concentrations. Burst release was observed in the first week with approximately 55% of DX leached from the polymeric implants. A sustained drug release was observed thereafter.

FTIR Analysis of the Degraded PUD Sheets

Fourier transform infrared spectrophotometer spectrum of the PUD sheets (without DX) showed typical absorption bands, such as carbonyl group of ester stretching vibration (~1730 cm^{-1}), nitrogen-hydrogen (N-H) bending vibration in secondary amide (~1640 cm^{-1}) (Fig. 2A), and -CH_2 stretching vibration (~2950 cm^{-1}) (Fig. 2B). Fourier transform infrared spectrophotometer of the degradation products of the PUD after 20 and 60 days incubation in PBS showed increased intensities of the bands at 1730 cm^{-1}, 1640 cm^{-1}, and 2950 cm^{-1}. An additional band at around ~3360 cm^{-1} corresponding to the free hydroxyl stretching vibrations was also observed (Fig. 2B).

In Vitro Cytotoxicity of the Degradation Products of the DX-PUD

The ARPE-19 cells were incubated in direct contact with the degradation products of the DX-PUD accumulated during 4 months in the PBS. After 1 and 4 days of incubation, the ARPE-19 cells showed 96.69 ± 2.27% and 91.1 ± 0.6% viability, compared to the control, respectively.

Biocompatibility of the DX-PUD Implanted in the SCS of Rat Eyes

The PUD sheets (with or without DX) were successfully inserted into the posterior and anterior SCS of the rat eyes (Figs. 3A, 3F), which was confirmed by the in vivo OCT examination (Fig. 3B). Fifteen days after polymer insertion, histologic cross section confirmed the presence of the polymeric implant in the posterior (Fig. 3F) or anterior SCS (Fig. 3C). Higher magnification showed that the structure of the retina over the implant was well preserved (Fig. 3D). No inflammatory cell infiltration was observed in the anterior segment of the rat eyes (Fig. 3E).

DX-PUD Limited the Severity of Uveitis

Dexamethasone-PUD sheets, containing 8% and 30% (wt/wt) of the drug, were inserted into the anterior SCS of the eyes 15 days before LPS challenge, so that a sustained release of DX was obtained in the eyes at the time of uveitis induction. Dexamethasone controlled released from the polymeric implants led to a significant reduction of the clinical intensity of the EIU as compared to the blank PUD and the control group (EIU), an effect comparable to DX delivered by subconjunctival or intravitreal injection (Fig. 4A). Polymeric implants loaded with 30% (wt/wt) DX were then used for the following experiments. Of note, even with this highest concentration, the PUD sheets contained only 0.07 mg DX.

Histologic analysis showed that DX controlled released from the PUD inhibited the inflammatory cell infiltration in the ocular tissues (Fig. 4D) when compared to the eyes receiving the blank PUD sheets (Fig. 4C) and to the eyes in the EIU control group (Fig. 4B). Quantification of inflammatory cells showed that DX leached from the PUD significantly reduced the number of PMN (Fig. 4E) and ED1-positive macrophages (Fig. 4F) when compared to the blank PUD and EIU control groups.

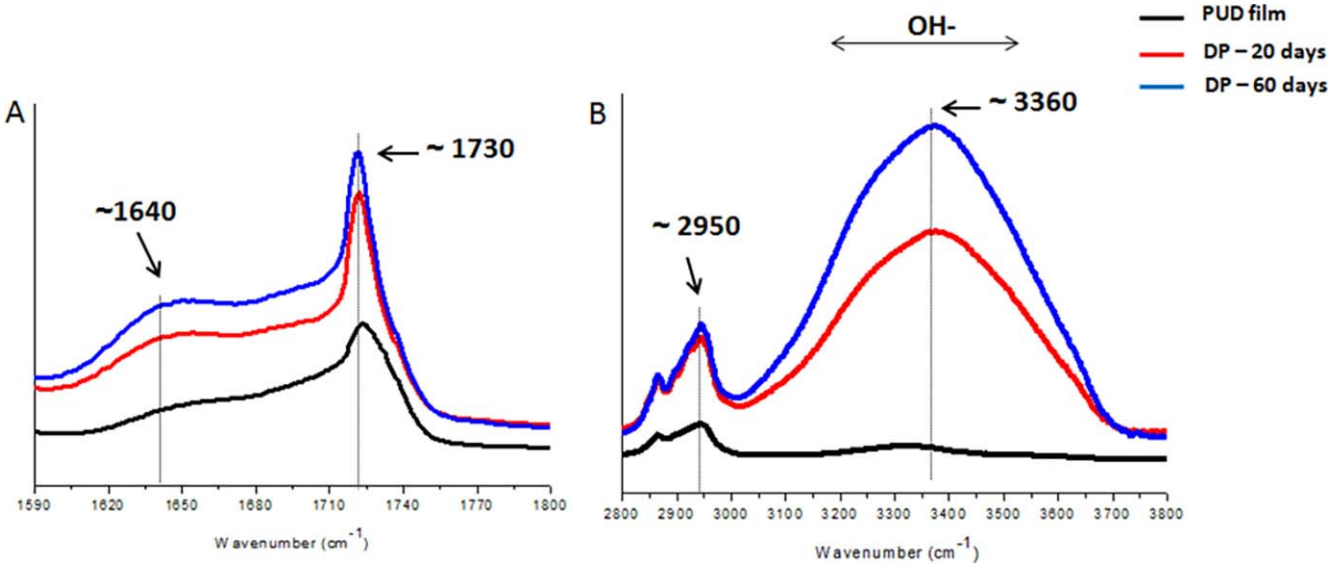

Figure 2. Fourier transform infrared spectrophotometer spectra of degraded PUD sheets collected after 20 and 60 days of incubation in PBS (**A**, **B**).

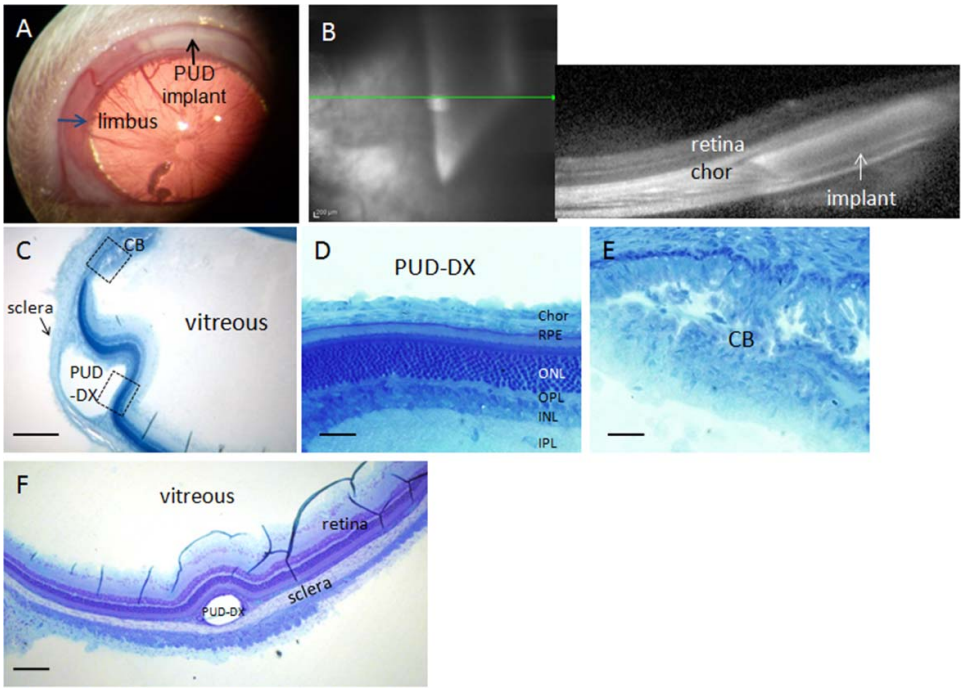

Figure 3. Ocular biocompatibility of the PUD and DX-PUD implants. (**A**) Biomicroscopy shows PUD sheet implanted behind the limbus (junction between the cornea and sclera) of the rat eye. (**B**) Optical coherence tomography performed on the same eye after surgery shows the position of the PUD implant in the suprachoroidal space under the peripheral retina. (**C**) Fifteen days after implantation, histologic section confirms the localization of the DX-PUD implant in the anterior suprachoroidal space close to the ciliary body (CB). (**D**) Higher magnification of the retinal area in the *lower rectangle* in (**C**) shows that the retina above the DX-PUD maintains its normal structure. (**E**) Higher magnification of the CB in the *upper rectangle* in (**C**) shows no inflammatory cell infiltration. (**F**) Retinal morphology remains normal 15 days after suprachoroidal implantation of DX-PUD in the posterior segment of the rat eye. *Scale Bars*: 200 μm (**C**, **F**); 20 μm (**D**, **E**). Chor, choroid; RPE, retinal pigment epithelium; ONL, outer nuclear layer; OPL, outer plexiform layer; INL, inner nuclear layer; IPL, inner plexiform layer.

DX-PUD Reduced Microglia/Macrophage Activation

To evaluate the effect of DX-PUD on microglia/macrophage activation and recruitment, we performed immunostaining with IBA-1 on cryostat sections. Round-shaped IBA-1–positive microglia/macrophage cells represent activated cells, while ramified IBA-1–positive microglia/macrophage cells are resting cells. In DX-PUD implanted eyes, most microglia/macrophages in the iris and ciliary body were ramified resting cells (Fig. 5C, inset), whereas in eyes implanted with blank PUD (Fig. 5B) and in nonimplanted eyes (Fig. 5A), microglia/macrophages were activated in the iris and ciliary body (arrows). Colabeling of IBA-1–positive cells with iNOS showed that iNOS was not expressed by microglia/macrophages in the eyes receiving the DX-PUD (Fig. 5C, inset). However, in the control groups, activated microglia/macrophages expressed iNOS (Figs. 5A, 5B, arrowheads in the insets).

DX-PUD and PUD Modified Cytokine Gene Expression

In the iris and ciliary body, DX-PUD downregulated the expression of *iNOS* and upregulated the expression of anti-inflammatory cytokine *IL-10* (Fig. 6A). Occludin transcripts were also increased with DX-PUD (not shown). However, no effect was observed on *IL-6* expression (Fig. 6A). In the retina, DX-PUD significantly reduced the transcripts of *IL-1β*, *IL-6*, and *CINC* compared to the EIU control group. However, the reduction of *iNOS* was not statistically significant (Fig. 6B). Noticeably, blank PUD also promoted the downregulation of *IL-6* and *iNOS* and upregulation of *IL-10* in the iris and ciliary body, and reduced *CINC* in the retina. The expression of TNF-α was not changed by DX-PUD (not shown).

Feasibility of PUD Implantation in Human Eyes

In order to show the feasibility of PUD implantation in human eyes, we used postmortem human eyes. After surgical insertion of PUD sheets (Fig. 7A–C), eyes were fixed immediately for histologic observation, which showed correct localization of the implant in the supraciliary space (Figs. 7D, 7E) as desired.

Discussion

The treatment of retinal diseases associated with macular edema requires intravitreal injections of biologics or steroids, allowing for high and prolonged drug concentration in the vitreous cavity. However, to maintain therapeutic drug concentration in the target site, repeated intravitreal injections are often required, which are often associated with poor compliance and discomfort, risks of vitreous hemorrhage, retinal detachment, intraocular pressure elevation,[19] cataract progression, endophthalmitis,[20,21] and ocular toxicity.[22]

The strategies to improve the bioavailability of drugs to the posterior segment of the eye and to minimize the risks of repeated intravitreal injections include the development of control-release intraocular drug-incorporated implants. In this study, we report a biodegradable PUD polymer releasing DX progressively and implanted in the anterior SCS of rat eyes that successfully limits the severity of EIU by decreasing the inflammatory cell infiltration, reducing the microglia/macrophage activation, and modulating the cytokine expression.

The polyurethane applied to design these implantable devices was synthesized using poly(caprolactone) (PCL) and poly(ethylene glycol) (PEG) as soft segment and urethane as hard segment. The hard segment provides dimensional stability

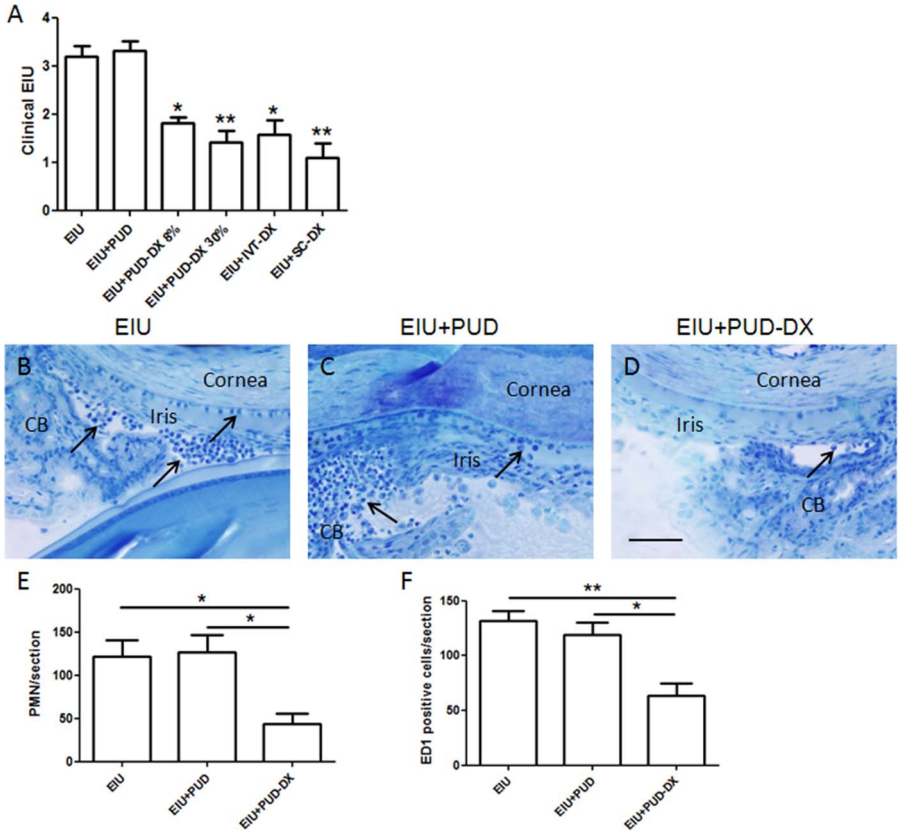

Figure 4. DX-PUD implants limit the severity of EIU in the rat eyes. (**A**) DX-PUD implants decrease the clinical score of uveitis 24 hours after LPS challenge in a dose-dependent manner. This effect is comparable to DX injected in the vitreous (IVT, 0.25 μg) or in the subconjunctival space (SC, 20 μg). $n = 13$ for EIU, 12 for EIU+PUD, 4 for EIU+DX-PUD 8% (wt/wt), 6 for EIU+DX-PUD 30% (wt/wt), 8 for EIU+IVT-DX, and 5 for EIU+SC-DX. (**B–D**) Histologic sections of rat eyes show infiltration of inflammatory cells (*arrows*) in the anterior segment of EIU (**B**) and PUD-implanted EIU eyes (**C**), while in DX-PUD implanted eyes, fewer inflammatory cells are observed. *Scale Bar*: 50 μm. CB, ciliary body. (**E**) Quantification of PMN leukocytes on histologic sections of rat eyes shows that DX-PUD implants reduce PMN infiltration as compared to PUD-implanted EIU eyes or EIU group ($n = 7$ rats per condition); (**F**) Quantification of ED1-positive macrophages on immunofluorescence sections shows that DX-PUD implants also decrease macrophage infiltration as compared to nonimplanted and PUD-implanted EIU eyes ($n = 4$ rats per condition). $^{*}P < 0.05$; $^{**}P < 0.01$.

by acting as reinforcing filler and as thermally reversible crosslink. The soft segment provides the elastomeric character to the polymer backbone.[23,24] The PCL presents labile aliphatic ester linkages, which can be hydrolyzed in the biological environment. However, degradation rate of PCL alone is rather slow due to its hydrophobicity and semicrystalline structure.[25] To accelerate polymer biodegradation, PEG can be introduced to increase hydrophilicity and aqueous absorption.[26,27] The

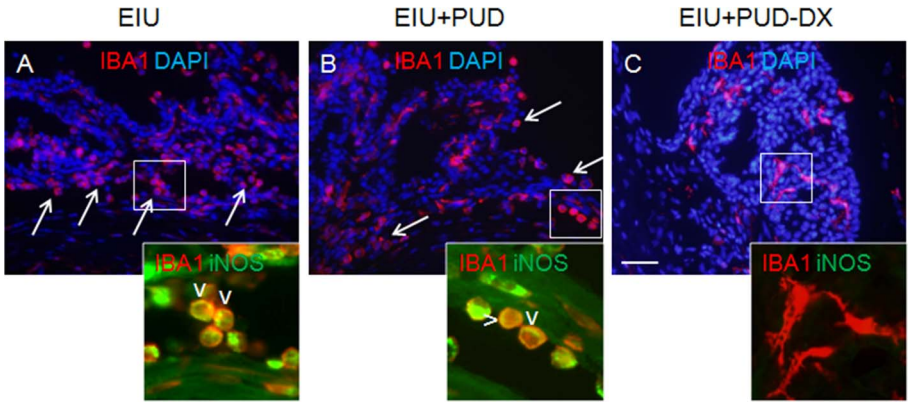

Figure 5. DX-PUD implants reduced microglia/macrophage activation in EIU rat eyes. (**A**) IBA-1 immunostaining (*red*) shows that in the EIU control group, most microglia/macrophages in the iris/ciliary body display a round shape (*arrows*), suggesting microglia/macrophage activation. Colabeling of IBA-1 with iNOS (*green*) shows that these round IBA-1–positive cells express iNOS (*inset*, *arrowheads*). (**B**) In the EIU eyes receiving blank PUD implants, most IBA-1–positive microglia/macrophages (*arrows*) are also in a round activated shape, colocalizing with iNOS (*inset, arrowheads*). (**C**) In the eyes receiving DX-PUD implants, most IBA-1–positive cells are in a resting ramified shape, and iNOS is not expressed by these cells (*inset*). *Scale Bar*: 20 μm.

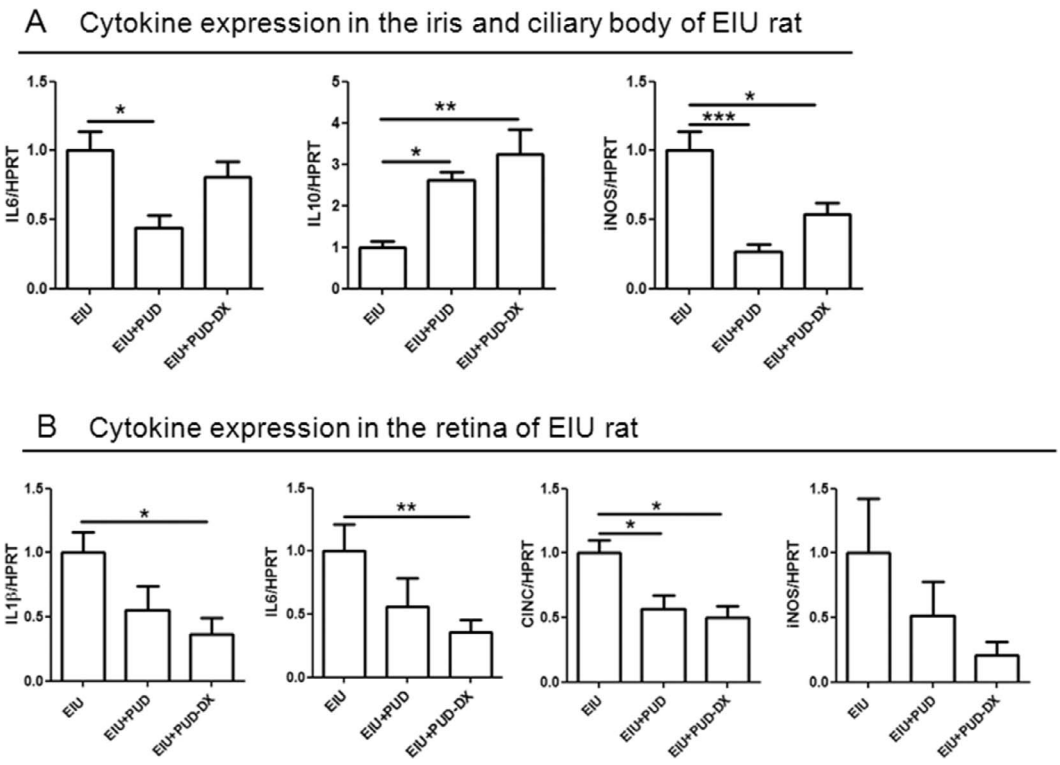

Figure 6. Quantitative PCR of cytokine expression in the iris/ciliary body and in the retina of EIU rats. (**A**) In the iris and ciliary body, DX-PUD implants downregulate the expression of *iNOS* and upregulate the expression of *IL-10*. Blank PUD implants downregulate the expression of *IL-6* and *iNOS* and upregulate the expression of *IL-10*. (**B**) In the retina, DX-PUD implants reduce significantly the transcripts of *IL-1β*, *IL-6*, and *CINC*; the decrease in *iNOS* mRNA is not significant. Blank PUD implants downregulate *CINC*. *HPRT* was used as housekeeping gene. Data are expressed relative to the EIU control ($n = 5$ rats per condition). $^{*}P < 0.05$; $^{**}P < 0.01$, $^{***}P < 0.001$.

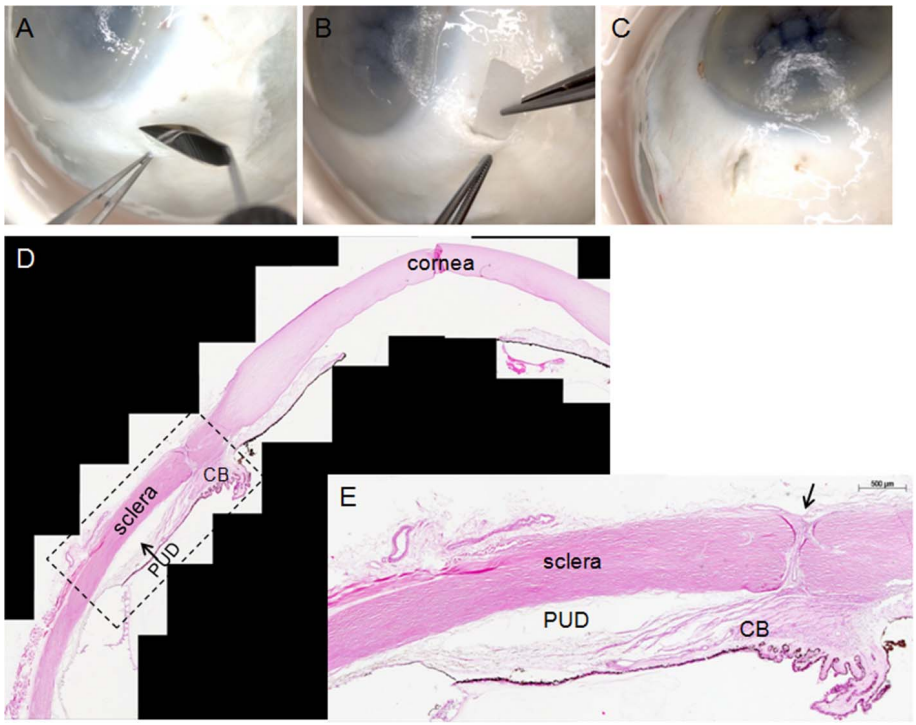

Figure 7. Supraciliary implantation of PUD in postmortem human eye. (**A–C**) Surgical procedure of supraciliary implantation of the PUD sheet. (**D**) Histology of the anterior segment of the implanted postmortem human eye shows that the PUD is located between the sclera and the pars plana of ciliary body (CB). (**E**) Higher magnification of the rectangle area in (**D**). *Arrow* in (**E**) indicates the sclera incision.

FTIR spectra of the degraded polyurethane after 20 and 60 days of incubation demonstrated the presence of an additional band at around 3360 cm^{-1}, equivalent to the free hydroxyl stretching vibrations, and the existence of an intensified band at around 1730 cm^{-1}, indicating the augmentation of free carbonyl groups. These bands could be attributed to the aqueous hydrolysis of the ester group of the PCL from 20 to 60 days, resulting in continuous formation of free carbonyl groups and hydroxyls associated to aliphatic groups (alcohol). Hydrolysis of the ester bonds further enhances the hydrophilic nature of the soft domains,[26] which increases their compatibility with the polar hard segments, leading to higher levels of mixing of these segments. As a consequence, the urethane linkages of the hard segments are deeply exposed to diffused water, inducing their hydrolysis, and possible chain scissions in the polyurethane. These cleavages are evidenced by the increased intensity of the secondary amide at around 1640 cm^{-1} present in the hard segments.

The degradation of PUD polymer is also an important characteristic that influences the release profile of the loaded drug, mainly when this drug is highly hydrophobic as is the DX. During the first 7 days, a burst release of approximately 55% DX from the implantable sheets was observed. In this stage, water penetrates into preexistent channels and pores of the polyurethane and dissolves the DX. The presence of hydrophilic PEG also helps water penetration.[15] From 8 to 42 days, a controlled and sustained release of DX from the polymer was achieved. During this period, higher aqueous diffusion induced by PEG in the soft segments leads to the hydrolysis of the ester bonds of the PCL in the soft segments and the urethane linkages in the hard segments, producing chain scissions of the polyurethane. As a result, new channels and pores connecting the surface to the inside of the matrix are generated for drug diffusion. Therefore, the PUD sheets controlled release the DX in a complex kinetic mechanism, involving the diffusion of the drug and erosion of the polymeric chains.

The DX-PUD sheets were submitted to a 4-month period of biodegradation, and the collected by-products have been shown to be noncytotoxic to ARPE-19 cells. The reagents applied as precursors of this polyurethane were carefully selected so that the hydrolytic biodegradation process was favorable, and the degradation by-products were previously supposed to be noncytotoxic to ARPE-19 cells.[26] Furthermore, DX is not supposed to present a significant degradation at the available conditions, since it is chemically stable after reconstitution in 0.9% saline injection for a long period.[28] The viability of ARPE-19 cells incubated with by-products of DX-PUD is comparable to that of cells incubated with by-products of blank PUD,[26] indicating nontoxicity of the accumulated DX released from PUD sheets. The biocompatibility of blank PUD has been previously shown in rat eyes after 15 days of suprachoroidal implantation.[13] We did not find additional retinal toxicity induced by DX released from PUD sheets.

Endotoxin-induced uveitis is a well-characterized rat model for mimicking the pathologic conditions in human acute uveitis. Footpad injection of LPS in Lewis rats induces an acute anterior uveitis involving also the posterior segment.[16,29] We chose to position the PUD sheet posterior to the limbus and just adjacent to the anterior uvea, where inflammation begins. The structure and physical properties of the material allow design of thin and foldable implant sheets that are rigid enough to serve as a guide for suprachoroidal implantation.

In EIU, infiltration of monocytes in the iris is observed as early as 2 hours after LPS injection, followed by a massive myeloid cell infiltration, mostly PMN, at 4 to 6 hours. After this initial peak, a massive infiltration of cells into the iris and ciliary body occurs at 24 hours.[30,31] Macrophages and neutrophils are the main source of the proinflammatory cytokines leading to anterior uveal inflammation and breakdown of the blood–aqueous barrier.[31] Tumor necrosis factor-α and IL-1 are produced early by resident macrophages/microglia responding to endotoxin. Tumor necrosis factor-α and IL-1 can induce IL-6, which contributes to the inflammation including activation of macrophages.[32] Cytokine-induced neutrophil chemoattractant is the rat equivalent of human IL-8, a CXC chemokine that is increased in aqueous humor at the time of cell infiltration.[33] Later in the course of EIU, anti-inflammatory cytokines including IL-10 participate in downregulation of proinflammatory mediators and inhibit inflammatory cell infiltration in EIU.[34] Continuous high expression of IL-10 in the eye has been also shown to play an important role in the mechanism of LPS tolerance in rat EIU.[35] Inducible NOS is produced by infiltrating neutrophils and monocytes and resident macrophages as well as by vascular endothelium. Nitric oxide (NO) synthesis by iNOS can also be induced by LPS or cytokines such as TNF-α and IL-1. Nitric oxide may contribute to breakdown of the blood–aqueous barrier during EIU.[31] We showed that PUD sheets releasing DX reduce EIU by preventing infiltration of polymorphonuclear cells and macrophages. Activation of macrophages/microglia is also inhibited with reduced production of iNOS by these cells. Dexamethasone-PUD sheets induce anti-inflammatory cytokines and inhibit production of proinflammatory cytokines and chemokines, contributing to prevention of uveitis. It is interesting that the blank PUD alone regulates cytokine and chemokine expression. Further investigations are required to identify the degradation products of PUD that may have anti-inflammatory potential.

Because the rat eye has anatomic characteristics far different from the human eye, we have also evaluated the feasibility of PUD implantation in the supraciliary space showing an easy access to this site. To target the posterior retina and choroid, such an implantation site might not be optimal; but for the treatment of uveitis, corticosteroids and/or immunosuppressive could be delivered locally very close to the uveal tissue.

In conclusion, biocompatible anterior suprachoroidal PUD sheets allow controlled release of incorporated DX that prevent inflammatory events of EIU. They could also be easily implanted into the SCS of the posterior segment to potentially target retinal/choroidal diseases.

Acknowledgments

Supported by Brazilian Government and Coordination of Improvement of Senior Staff (CAPES, Bolsistas da CAPES, Brasília, Brazil), National Council for Scientific and Technological Development (CNPq, Bolsistas do CNPq, Brasília, Brazil), Fundation de Amparo a Pesquisa do Estado de Minas Gerais (FAPEMIG, Minas Gerais, Brazil), French Institute of Health and Medical Research (INSERM), and a CNPq grant of Brazil (Bolsistas do CNPq, Brasilia, Brazil) (JBS).

Disclosure: **J. Barbosa Saliba**, None; **L. Vieira**, None; **G.M. Fernandes-Cunha**, None; **G. Rodrigues Da Silva**, None; **S. Ligório Fialho**, None; **A. Silva-Cunha**, None; **E. Bousquet**, None; **M.-C. Naud**, None; **E. Ayres**, None; **R.L. Oréfice**, None; **M. Tekaya**, None; **L. Kowalczuk**, None; **M. Zhao**, None; **F. Behar-Cohen**, None

References

1. Gaudana RJ, Ananthula HK, Parenky A, Mitra AK. Ocular drug delivery. *AAPS J.* 2010;12:348–360.
2. Chen P, Chen H, Zang X, et al. Expression of efflux transporters in human ocular tissues. *Drug Metab Dispos.* 2013;41:1934–1948.

3. Haller JA, Bandello F, Belfort R Jr, et al. Randomized, sham-controlled trial of dexamethasone intravitreal implant in patients with macular edema due to retinal vein occlusion. *Ophthalmology*. 2010;117:1134–1146.
4. Lowder C, Belfort R Jr, Lightman S, et al. Dexamethasone intravitreal implant for noninfectious intermediate or posterior uveitis. *Arch Ophthalmol*. 2011;129:545–553.
5. Dugel PU, Bandello F, Loewenstein A. Dexamethasone intravitreal implant in the treatment of diabetic macular edema. *Clin Ophthalmol*. 2015;9:1321–1335.
6. Jaffe GJ, Martin D, Callanan D, et al. Fluocinolone acetonide implant (Retisert) for noninfectious posterior uveitis: thirty-four-week results of a multicenter randomized clinical study. *Ophthalmology*. 2006;113:1020–1027.
7. Zucchiatti I, Lattanzio R, Querques G, et al. Intravitreal dexamethasone implant in patients with persistent diabetic macular edema. *Ophthalmologica*. 2012;228:117–122.
8. Zarranz-Ventura J, Carreño E, Johnston RL, et al. Multicenter study of intravitreal dexamethasone implant in noninfectious uveitis: indications, outcomes, and reinjection frequency. *Am J Ophthalmol*. 2014;158:1136–1145.
9. Kang-Mieler JJ, Osswald CR, Mieler WF. Advances in ocular drug delivery: emphasis on the posterior segment. *Expert Opin Drug Deliv*. 2014;11:1647–1660.
10. Olsen TW, Feng X, Wabner K, et al. Cannulation of the suprachoroidal space: a novel drug delivery methodology to the posterior segment. *Am J Ophthalmol*. 2006;142:777–787.
11. Patel SR, Berezovsky DE, McCarey BE, et al. Targeted administration into the suprachoroidal space using a microneedle for drug delivery to the posterior segment of the eye. *Invest Ophthalmol Vis Sci*. 2012;53:4433–4441.
12. Gilger BC, Abarca EM, Salmon JH, Patel S. Treatment of acute posterior uveitis in a porcine model by injection of triamcinolone acetonide into the suprachoroidal space using microneedles. *Invest Ophthalmol Vis Sci*. 2013;54:2483–2492.
13. Da Silva GR, Junior AS, Saliba JB, et al. Polyurethanes as supports for human retinal pigment epithelium cell growth. *Int J Artif Organs*. 2011;34:198–209.
14. Moura SA, Lima LD, Andrade SP, et al. Local drug delivery system: inhibition of inflammatory angiogenesis in a murine sponge model by dexamethasone-loaded polyurethane implants. *J Pharm Sci*. 2011;100:2886–2895.
15. Da Silva GR, Da Silva Cunha A, Ayres E, Oréfice RL. Effect of the macromolecular architecture of biodegradable polyurethanes on the controlled delivery of ocular drugs. *J Mater Sci Mater Med*. 2009;20:481–487.
16. Rosenbaum JT, McDevitt HO, Guss RB, Egbert PR. Endotoxin-induced uveitis in rats as a model for human disease. *Nature*. 1980;286:611–613.
17. El Zaoui I, Touchard E, Berdugo M, et al. Subconjunctival injection of XG-102, a c-Jun N-Terminal Kinase inhibitor peptide, in the treatment of endotoxin-induced uveitis in rats. *J Ocul Pharmacol Ther*. 2015;31:17–24.
18. Bousquet E, Zhao M, Ly A, et al. The aldosterone-mineralocorticoid receptor pathway exerts anti-inflammatory effects in endotoxin-induced uveitis. *PLoS One*. 2012;7:e49036.
19. Sonmez K, Ozturk F. Complications of intravitreal triamcinolone acetonide for macular edema and predictive factors for intraocular pressure elevation. *Int J Ophthalmol*. 2012;5:719–725.
20. Ozkiriş A, Erkiliç K. Complications of intravitreal injection of triamcinolone acetonide. *Can J Ophthalmol*. 2005;40:63–68.
21. Moshfeghi AA. Endophthalmitis following intravitreal anti-vascular endothelial growth factor injections for neovascular age-related macular degeneration. *Semin Ophthalmol*. 2011;26:139–148.
22. Valamanesh F, Berdugo M, Sennlaub F, et al. Effects of triamcinolone acetonide on vessels of the posterior segment of the eye. *Mol Vis*. 2009;8:2634–2648.
23. Coutinho FMB, Delpech MC. Degradation profile of films cast from aqueous polyurethane dispersion. *Polym Degrad Stab*. 2000;70:49–57.
24. Ayres E, Oréfice RL, Yoshida MI. Phase morphology of hydrolysable polyurethanes derived from aqueous dispersions. *Eur Polym J*. 2007;43:3510–3521.
25. Zhang C, Zhang N, Wen X. Synthesis and characterization of biocompatible, degradable, light curable, polyurethane-based elastic hydrogels. *J Biomed Mater Res*. 2007;82:637–650.
26. Da Silva GR, Silva-Cunha A, Behar-Cohen F, Ayres E, Oréfice RL. Biodegradation of polyurethanes and nanocomposites to non-cytotoxic degradation products. *Polym Degrad Stab*. 2010;95:491–499.
27. Guan J, Sacks MS, Beckman EJ, Wagner WR. Biodegradable poly(ether ester urethane)urea elastomers based on poly(ether ester) triblock copolymers and putrescine: synthesis, characterization and cytocompatibility. *Biomaterials*. 2004;25:85–96.
28. Lugo RA, Nahata MC. Stability of diluted dexamethasone sodium phosphate injection at two temperatures. *Ann Pharmacother*. 1994;28:1018–1019.
29. Yang P, de Vos AF, Kijlstra A. Macrophages in the retina of normal Lewis rats and their dynamics after injection of lipopolysaccharide. *Invest Ophthalmol Vis Sci*. 1996;37:77–85.
30. McMenamin PG, Crewe J. Endotoxin-induced uveitis. Kinetics and phenotype of the inflammatory cell infiltrate and the response of the resident tissue macrophages and dendritic cells in the iris and ciliary body. *Invest Ophthalmol Vis Sci*. 1995;36:1949–1959.
31. Smith JR, Hart PH, Williams KA. Basic pathogenic mechanisms operating in experimental models of acute anterior uveitis. *Immunol Cell Biol*. 1998;76:497–512.
32. Akira S, Hirano T, Taga T, Kishimoto T. Biology of multifunctional cytokines: IL6 and related molecules (IL1 and TNF). *FASEB J*. 1990;4:2860–2867.
33. Guex-Crosier Y, Wittwer AJ, Roberge FG. Intraocular production of a cytokine (CINC) responsible for neutrophil infiltration in endotoxin induced uveitis. *Br J Ophthalmol*. 1996;80:649–653.
34. Hayashi S, Guex-Crosier Y, Delvaux A, Velu T, Roberge FG. Interleukin 10 inhibits inflammatory cells infiltration in endotoxin-induced uveitis. *Graefes Arch Clin Exp Ophthalmol*. 1996;234:633–636.
35. Mashimo H, Ohguro N, Nomura S, et al. Neutrophil chemotaxis and local expression of interleukin-10 in the tolerance of endotoxin-induced uveitis. *Invest Ophthalmol Vis Sci*. 2008;49:5450–5457.

Investigative Ophthalmology & Visual Science